Available online at www.sciencedirect.com
SCIENCE DIRECT®
Applied Catalysis A: General 255 (2003) 181–195
APPLIED CATALYSIS A: GENERAL
www.elsevier.com/locate/apcata

Infrared study of the adsorption of formic acid on clean and Ca-promoted Pd/SiO_2 catalysts

Griselda C. Cabilla, Adrian L. Bonivardi, Miguel A. Baltanás*

INTEC—Instituto de Desarrollo Tecnológico para la Industria Química, (Universidad Nacional del Litoral, Consejo Nacional de Investigaciones Científicas y Técnicas), Güemes 3450, Santa Fe S3000GLN, Argentina

Received 20 March 2003; received in revised form 19 June 2003; accepted 3 July 2003

Abstract

The adsorption and decomposition of formic acid on a highly dispersed supported Pd/SiO_2 catalyst (2 wt.% Pd) prepared via ion exchange (IE) of $[Pd(NH_3)_4]^{2+}$ in alkaline solution, together with two Ca-promoted preparations (Ca/Pd = 2 at./at.) where calcium was added either to the prereduced Pd crystallites or to the diammine palladium complex, were studied by FTIR at 298–653 K.

On the support, HCOOH is mostly adsorbed molecularly at room temperature, with partial dimerization, condensation and extensive hydrogen bonding, but readily decomposes, on the Pd crystallites of Pd/SiO_2, via decarbonylation, to give CO multicoordinated to the metal surface, and water. With heating, formic acid decomposition is accompanied by some water gas shift as well, while CO reacts to give methyl (methane) and methoxy.

Calcium promotion to both the prereduced Pd and its diammine complex precursor, enhanced HCOOH decomposition onto the catalyst surface, even at 298 K. Together with sorbed HCOOH and chemisorbed CO, mono- and bidentate formates were observed on these materials, owing to the incorporation of well-dispersed CaO_xH_y. These formates were readily decomposed by atomic hydrogen produced by decarbonylation/WGS of formic acid on Pd. At increasing temperatures, some carbonates (polydentate and simple) were formed, but hardly any methane was detected. On Ca–Pd/SiO_2 with calcium added to prereduced Pd metal particles the extension and/or onset of all these processes was more straightforward than on the promoted Ca–Pd/SiO_2 where calcium was added to diammine palladium instead, most likely owing to the combined impact of a higher dispersion of the Pd crystallites on the former preparation, and calcium oxyhydroxide decoration (CaO_xH_y) of the metal particles on the latter, which hamper H-spillover from them.
© 2003 Elsevier B.V. All rights reserved.

Keywords: Syn-gas conversion; CO_2 hydrogenation; FTIR spectroscopy; Supported palladium; Calcium promotion; Formic acid adsorption

1. Introduction

Carboxylate species have been proposed as intermediates in a number of syngas-related catalytic processes. For example, one well-known mechanism for oxygenate synthesis from CO and H_2 over group VIII metal catalysts envisions the participation of stable carboxylates that undergo hydrogenation to yield alcohols [1]. This proposition was supported by IR spectra showing the presence of formate [1] and acetate [2] species during the course of methanol and ethanol synthesis, respectively, over these catalysts. As Lunsford has properly pointed out, while carboxylate formation is clearly not the only or major-pathway for oxygenate

* Corresponding author. Tel.: +54-342-455-9175; fax: +54-342-455-0944.
E-mail address: tderliq@ceride.gov.ar (M.A. Baltanás).

0926-860X/$ – see front matter © 2003 Elsevier B.V. All rights reserved.
doi:10.1016/S0926-860X(03)00546-5

synthesis from CO and H_2, the participation of these intermediates may be favorable for reactions occurring on group-VIII metal catalysts supported on certain metal oxides [3].

Even so, although these intermediates are frequently detected on supported metal catalysts, their location, their origin, and their contribution to the conversion of reactants to products remain to be defined. In the case of methanol synthesis with palladium catalysts, for example, both the Tamaru and co-workers [1] and Ponec and co-workers [4] groups proposed that Pd^0 does not produce methanol. The latter found a positive correlation between methanol synthesis activity and the concentration of extractable Pd^+ ions on the catalyst, while Tamaru's group correlated methanol synthesis activity with the population of formate species (detected by IR) which might be expected to be formed at such oxidized metal centers. Later reports, however, questioned these conclusions [5–7]. Studies on palladium single crystals showed that Pd^0 can make methanol from CO and H_2, but also that methanol decomposition to $CO + H_2$ (and by inference from microscopic reversibility, methanol synthesis) does not proceed via formates on clean palladium [7]. These observations implicate the oxide support rather than the metal as the binding site of the formate species detected spectroscopically, even though the site of their formation and the extent of their participation in the overall reaction scheme are less easily resolved.

Likewise, as regards the surface interaction between H_2 and CO_2 over palladium on various supports (SiO_2, MgO, TiO_2 and Al_2O_3), Solymosi et al. concluded that the formate ion formed in the surface reaction is located on the support: the hydrogen activated on the Pd spills over the support and reacts with hydrocarbonate to yield formate ion [8].

Certainly, both carbon oxides, CO and CO_2, can be selectively hydrogenated to methanol on supported palladium catalysts [9]. However, on pure or well-purified silica the catalytic activity of Pd/SiO_2 is rather poor, quite similar to that of Pd black [10,11]. Adding a suitable promoter to the system, such as Ca, has been shown to increase noticeably its catalytic activity and, also, its selectivity to methanol [11–14]. Thus, by incorporating calcium acetate or calcium nitrate (decomposable salts that will not lead to anionic promotion) to air-precalcined Pd/SiO_2, reaction rates up to 40-fold higher than with the unpromoted catalysts were achieved, using syn-gas mixtures at 2.5–3 MPa and usual process temperatures (523–553 K) [11,12].

Because the mechanism of methanol synthesis from $CO–CO_2–H_2$ mixtures over promoted Pd catalysts remains uncertain, current studies aim at improving the understanding of why the promoters are effective and, in particular, where they are located. Among these studies, a thorough evaluation of the nature of the possible reaction intermediates can contribute significantly to this knowledge and, to this end, the present work examines the adsorption and reaction of HCOOH on pure and Ca promoted Pd/SiO_2 by means of FTIR spectroscopy.

2. Experimental

A highly dispersed Pd/SiO_2 catalyst (2 wt.% Pd), together with two Ca-promoted preparations (Ca/Pd = 2 at./at.) and blanks of pure and calcium-loaded silica were used (Table 1). The catalysts were obtained via ion exchange (IE) of $[Pd(NH_3)_4]^{2+}$, prepared from 99.5 wt.% palladium acetate (Engelhard), on pre-purified, calcined Davison G-59 silica. Ion exchange was done at pH = 11 and 298 K (hereafter, room temperature, or RT), in aqueous solution. After washing at same pH, the ion-exchanged silica was dried in air at RT during 24 h. Support characterization and IE procedures have been fully reported in previous work [17].

After drying, the anchored Pd tetraammine complex was decomposed to the diaammine one at 423 K. Part of the stock was used as such, to prepare a first type of Ca-promoted catalysts (S code) where maximum Ca–Pd interaction was expected, while a second part was H_2 reduced instead at 723 K (2 K/min; 2 h), to minimize said interaction (R code). Calcium acetate was added to each material by pore volume impregnation, in vacuo, and then water was sublimated. Lastly, the catalysts were calcined at 673 K (2 K/min; 2 h) in dry, CO_2-free air and reduced in H_2 at 723 K. The percent exposed metal fraction (FE) of palladium was determined by using H_2 chemisorption at 298 K, and controlled with XRD and TEM. Further details can be found elsewhere [13,16].

Self-supporting wafers of the dried powders (10 mg/cm^2) were placed in a portable Pyrex flow-type

Table 1
Characteristics and codes of the catalysts

Catalyst type[a]	Pd loading (% Pd w/w)	Ca loading (% Ca w/w)	Ca/Pd (at./at.)	FE[b]	d_p (TEM)[c] (Å)	Code
R	2	1.5	2	0.65	1.4	MR5
S	2	–	0	0.75	1.5	MS0
	2	1.5	2	0.41	1.4–3.5[d]	MS5
Blank		1.5	NA			BS5
		–	NA			SiO_2

[a] Support: Davison G-59 silica, mesoporous ($S_g = 254\,m^2/g$; modal radius = 83 Å).
[b] Fraction of exposed Pd (hydrogen chemisorption). Chemisorption stoichiometry: $H_{ad}/Pd_s = 1$ [15].
[c] Average volume-to-surface particle diameters determined by transmission electron microscopy, where $d_p\,(TEM) = \sum n_i d_i^3 / n_i d_i^2$ [13,16].
[d] Bimodal distribution.

IR cell attached to a conventional high-vacuum system and a manifold, to allow for in situ pretreatments. Each catalyst wafer was reduced under flowing H_2 (100 cm^3/min) for 60 min at 523 K (2 K/min) after purging the cell with nitrogen, at RT, for 15 min. Sorbed hydrogen on Pd was eliminated by evacuation at 653 K (10 K/min; 2 h). The sample was subsequently cooled to RT. Background IR spectra of these 'clean' samples were obtained at each temperature, for their further substraction.

Formic acid (Carlo Erba, 99% RPE), previously outgased by a series of freeze-thaw cycles under vacuum, was stored in a glass bulb and dosed into the cell (1 Torr) at RT. The sample was so kept for 30 min and spectra were taken every 5 min. Next, the temperature was raised to 653 K (3 K/min), with additional IR spectra taken every 20 K. Then, the cell was evacuated to 3×10^{-5} Torr; intermediate spectra were recorded at 1, 10^{-1}, 10^{-2}, 10^{-3} and 10^{-4} Torr. Lastly, the temperature was lowered to 523 K and H_2 flown through the cell (60 cm^3/min), to record the reactive behavior (or desorption) of any species that might remain after the evacuation at high temperature. For comparison purposes, the gas phase spectra of HCOOH (1 Torr) at each temperature was recorded and substracted wherever necessary.

The transmission spectra were taken with a single beam Shimadzu 8001 FTIR spectrometer ($R = 4\,cm^{-1}$; 100 scans per spectrum). Background spectra of the clean samples, obtained at each temperature, were subtracted; background noise correction and Gaussian deconvolution of bands were done on digitized spectra, using the Microcal Origin® 4.1 software package.

Gas sources were 99.999% N_2 and H_2 (Scott U.P.G.), purified to remove water and oxygen with 3 Å molecular sieve and MnO/Al_2O_3 cartridges, respectively.

3. Results and discussion

3.1. Adsorption/desorption of formic acid on the reference materials

3.1.1. SiO_2

Formic acid readily adsorbs onto silica at ambient temperature. After 30 min exposure to 1 Torr HCOOH the spectral features very much resembled the initial ones (Fig. 1) and were almost identical to those reported by Millar et al. [18]. In the high frequency region several bands appeared at 3064, 2939, 2727 and 2572 cm^{-1}. The first two signals have been assigned to the ν(OH) of the acid dimer and the ν(CH) of the physisorbed HCOOH molecule, respectively [18,19], while the remaining bands belong to ν(OH) of condensed HCOOH hydrogen-bonded to the surface [20].

The most characteristic bands of formic acid physisorbed onto silica at RT appear in the low frequency region: CO-stretching, at 1725 cm^{-1} [8,18,21,22], together with the partially convoluted signals located at 1390 cm^{-1} [δ(CH)] and 1357 cm^{-1} [ν_s(OCO)] [18,22–25] (Fig. 1). Some HCOOH(g) was also

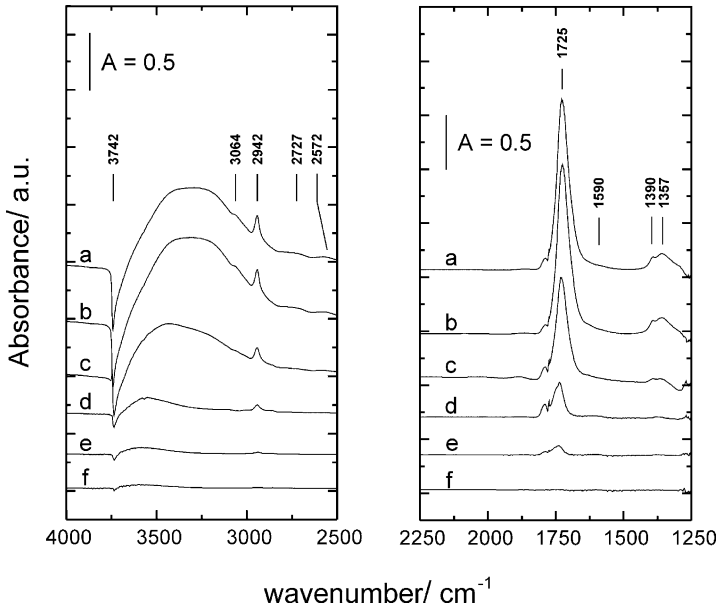

Fig. 1. FTIR spectra of formic acid (1 Torr) adsorbed on SiO_2 (Davison G-59) at increasing temperatures: (a) 298 K, 0.5 min; (b) 298 K, 30 min; (c) 333 K; (d) 473 K; (e) 573 K and (f) 653 K, 30 min (spectra were taken at the temperatures noted). The-sample was prereduced in situ under flowing H_2 (523 K; 1 h), evacuated (653 K; 2 h) and cooled down to RT.

present in the cell, as indicated by the tiny shoulders at 1791 and 1775 cm^{-1} (R and Q branches of ν_s(C=O) [26,27]).

The asymmetry of the 1725 cm^{-1} band toward shorter wavenumbers suggests that a little bidentate formate (b-HCOO) was formed on the surface at 298 K as well. The fingerprint vibration of this species, ν_{as}(OCO), which is usually found at 1590–1598 cm^{-1} and whose frequency is practically independent of the adsorbent [23–25,28–33], can be recognized above 473 K (see later). Its remaining fingerprint vibration, ν_s(OCO), at 1357 cm^{-1}, is convoluted with molecular, physisorbed HCOOH [18], which also has a δ(CH) mode at 1390 cm^{-1}.

The OH region reveals extensive hydrogen bonding, as shown by the broad band about 3450–3250 cm^{-1} and the intense negative peak at 3742 cm^{-1}, which indicates that isolated OH groups of the silica were consumed (isolated hydroxyl groups are left on the silica after the high temperature evacuation pretreatment). These features of the adsorption process of HCOOH on the support can be represented by the following scheme:

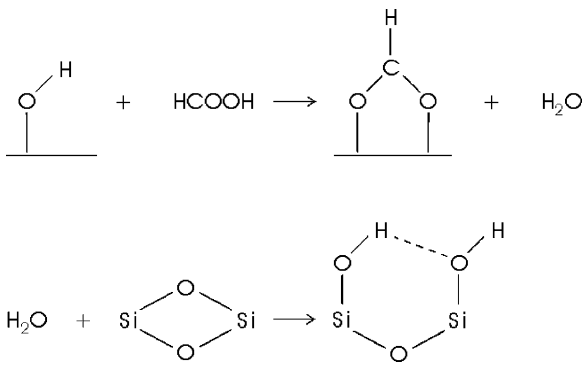

Upon heating all the IR bands progressively disappeared (Fig. 1). During this process, the acid dimer converted into the monomer. So, the δ(OH) signal at 3060 cm^{-1} dimmed away and the broad 3450–3250 cm^{-1} band turned asymmetric. At 653 K the spectrum became almost flat.

The free OH groups of the silica surface, lost during exposure to the adsorbate at room temperature, regenerated almost entirely on heating. At 653 K 95% of these hydroxyls were recovered, which seems to be a

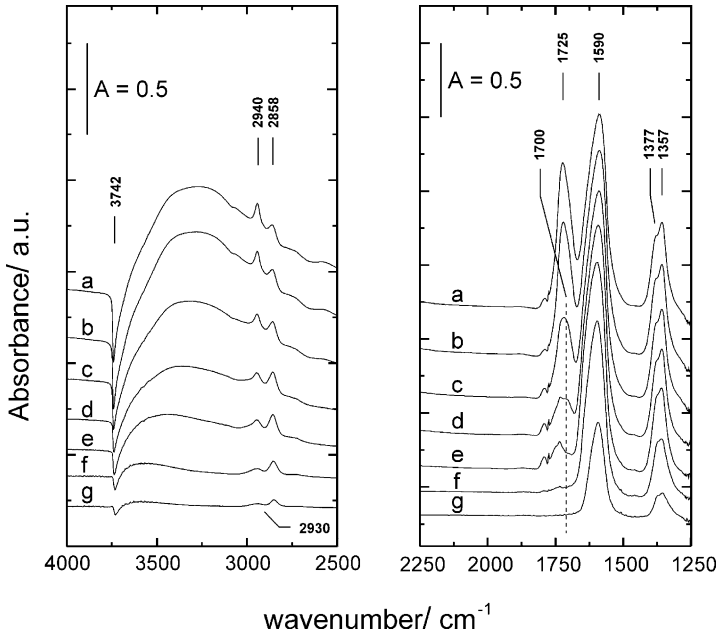

Fig. 2. Infrared spectra of HCOOH (1 Torr) adsorbed on BS5 (blank of Ca/SiO_2) at increasing temperatures: (a) 298 K, 0.5 min; (b) 298 K, 30 min; (c) 333 K, (d) 373 K, (e) 433 K; (f) 573 K and (g) 653 K, 30 min. The sample was pretreated as indicated in Fig. 1.

typical behavior of the adsorption and weak interaction of carboxylic acids onto silica [34].

3.1.2. CaO_x/SiO_2

As shown in Fig. 2, the exposure of the calcium-added silica to 1 Torr HCOOH at 298 K gave dramatically different spectra. The bands corresponding to formic acid physisorbed onto SiO_2 were smaller than on the bare support and decreased with time while, simultaneously, two bands located at 2858 cm^{-1} [ν(CH)] and at 1590 cm^{-1} [ν_{as}(OCO)], both typical of b-HCOO, grew larger. The 1590 cm^{-1} signal of bidentate formate, in fact, dominates the IR spectrum of CaO_x/SiO_2 thus revealing the extent of the acid–base surface reaction on the added calcium oxyhydroxide CaO_xH_y [13]. Concurrently, the bands at 1378 and 1357 cm^{-1}, also assigned to chemisorbed b-HCOO [18], were much more prominent than on SiO_2. The signals of the dimer and condensed formic acid onto silica, as well as the tiny bands given by the R and Q branches of the ν_s(C=O) vibration of HCOOH(g) were also recognizable at RT. The consumption of isolated hydroxyls of the silica (i.e. the negative peak at 3742 cm^{-1}) was about 45% smaller than on the pure support, which might further indicate that the added CaO_xH_y is well-dispersed.

On heating, most of these free OH groups were regenerated (Fig. 2), while the high frequency bands at 2940–2930 (broad, convoluted) and 2858 cm^{-1} became much smaller, but still clearly detectable. At 653 K these signals were 10 times stronger on the calcium-added SiO_2 than on the pure support. The 2930 cm^{-1} band is a combination mode [$\nu_{comb} = \nu_{as}(OCO) + \delta(CH)$] of bidentate formate [18,35,36].

In like manner, all the bands in the CO stretching region decreased with heating, but the signals related to b-HCOO groups (1590, 1377 and 1357 cm^{-1}) remained quite strong even at the highest temperature. The asymmetry on the high-frequency side of the 1590 cm^{-1} band up to 433 K suggests the presence of some molecular water (viz. δ(HOH) at 1630 cm^{-1}). The ν(CO) of HCOOH physisorbed on silica was no longer observable above 573 K.

The heating process revealed that some monodentate formate (hereafter m-HCOO) had also been formed on the surface at RT, as the 1725 cm^{-1} peak of physisorbed formic acid was broadened to the low-frequency side and at 373 K another

absorbance maximum, corresponding to the characteristic ν_{as}(OCO) band of m-HCOO (1700 cm^{-1} [27,37]) became explicit (Fig. 2). The species was no longer appreciable above 573 K, though.

Evacuation at 653 K eliminated about 30% of the surface formates. Both, the high and low frequency bands, decreased proportionally. The reactivity of these surface HCOO groups upon exposure to flowing H_2 at 523 K was modest, with at most 15% of additional consumption/desorption after 1 h onstream.

3.1.3. Pd/SiO_2

Formic acid is stable on metal surfaces only at low temperature [38]. Consequently, HCOOH adsorbs and reacts at 298 K on Pd/SiO_2 (Fig. 3). Unlike the case of pure silica, and because part of the dosed HCOOH was decomposed rather than just sorbed, fewer free hydroxyls were consumed on Pd/SiO_2. At low temperature, the decarbonylation channel is favored [39].

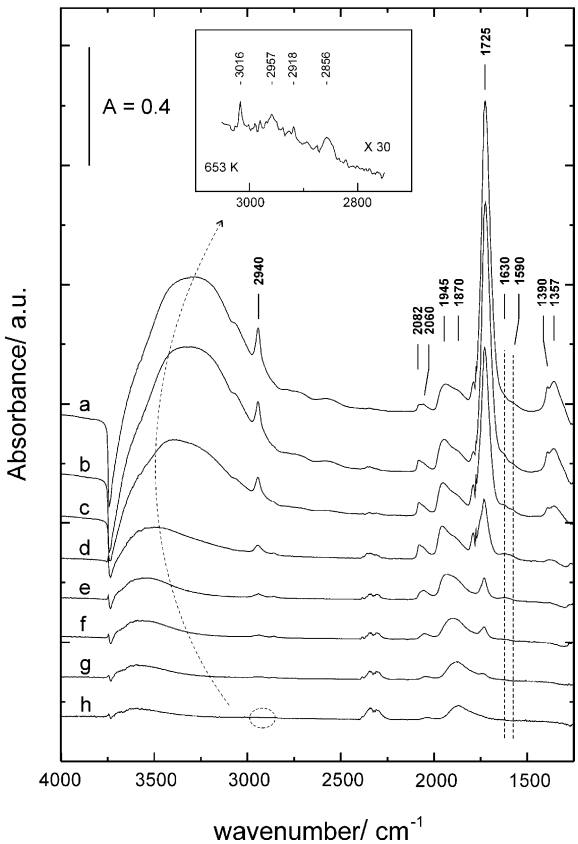

Fig. 3. FTIR spectra of HCOOH (1 Torr) adsorbed on Pd/SiO_2 at increasing temperatures: (a) 298 K, 0.5 min; (b) 298 K, 30 min; (c) 333 K; (d) 373 K; (e) 433 K; (f) 493 K, (g) 573 K and (h) 653 K, 30 min. The sample was pretreated as described in Fig. 1.

$$HCOOH \rightarrow CO + H_2O \quad (1)$$

So, while each of the absorption bands shown by HCOOH adsorption on silica were again recognizable upon exposure of Pd/SiO_2 to 1 Torr HCOOH, their intensity was lower than on the bare support (about 50% smaller at $t = 0.5$ min) and became even smaller with time (Fig. 3). Concurrently, the characteristic bands of chemisorbed CO grew up, with maxima located at 2082, 2060, 1945 and 1870 cm^{-1}. The decomposition of HCOOH via Reaction (1) is also revealed by the δ(HOH) band of condensed, molecular water (1630 cm^{-1}).

Bands above 2000 cm^{-1} are attributed to terminal, mono-coordinated or linearly bonded carbon monoxide (CO_L,) while the broad, convoluted bands under 2000 cm^{-1} are assigned to multicoordinated CO. From single crystal studies, the latter have been further classified as: CO_{B1}, corresponding to di-coordinated CO on structurally open planes, such as (100) or (210), close to 1970 cm^{-1}, CO_{B2}, corresponding to di-coordinated CO on Pd(111), around 1956 cm^{-1} and a band below 1830 cm^{-1} usually assigned to triply bridging CO on Pd(1 1 1) "hollow" sites, CO_H. On supported palladium these bands locate at lower frequencies than on Pd single crystals [40]. In our sample CO_L linearly bonded to both, planes and edges and corners (2082 and 2060 cm^{-1}, respectively), represented a fair size of the total, thus revealing the high dispersion of the metal.

Both desorption and decomposition of the sorbed formic acid progressed upon heating (Fig. 3). Nevertheless, some physisorbed HCOOH was still appreciable at 573 K (see the prominent signal of ν(CO) at 1725 cm^{-1}). At 333 K, the tiny band at 2856 cm^{-1} in the ν(CH) region, together with an accompanying, well resolved signal at 1590 cm^{-1}, are a telltale of the presence of a few b-HCOO on the surface. The HCOOH decomposition is accompanied by the water gas shift reaction (WGSR).

$$CO + H_2O \leftrightarrow CO_2 + H_2 \quad (2)$$

Accordingly, the characteristic 2349 cm^{-1} band of CO_2(g) also appears in the spectra (Fig. 3). Hydrogen, in turn, can reduce b-HCOO to stable methoxy

groups, which chemisorb onto silica giving bands at 2957 [$\nu_{as}(CH_3)$] and 2857 [$\nu_s(CH_3)$] cm^{-1} superimposed with those of formate.

$$HCOO^- + 2\,H_2 \rightarrow H_3CO^- + H_2O \quad (3)$$

Methoxy groups, which can form onto silica above 253 K upon exposing it to methanol, are very stable and cannot be removed by heating [28,41]. At low pressure and commercial process conditions ($T > 523$ K), though, the preferred hydrogenation route on well-dispersed Pd/SiO_2 catalysts leads to methane [37], as indicated by the signal of CH_4(g) at 3016 cm^{-1} [19] and the C–H stretching of methyl groups chemisorbed onto Pd, at 2920 cm^{-1} [42]. At 653 K, further progress of the WGSR is appreciable (from the additional buildup of CO_2) as well (Fig. 3, trace h).

The integrated intensity of the ν(CO) signals of carbon monoxide chemisorbed onto Pd grew up to 393 K, and became progressively smaller at higher temperatures, where the desorption/reaction of CO was faster than HCOOH decomposition. This maximum agrees well with the desorption maxima of chemisorbed CO (400 K) reported by different authors for either Pd or Rh [20,43]. Linearly bonded CO_S desorbs more easily than di-coordinated species; some of the latter, bonded to palladium in low-index planes (CO_{B2}) still remained chemisorbed at 653 K. In addition, the spectral location of all these ν(CO) bands shifted noticeably on heating. This well-known phenomenon can be attributed both to changes in the preferred adsorption forms and relative stability with temperature of the different adsorbed modes of CO and to changes in the dipole–dipole coupling of the adsorbate; with desorption, the latter becomes less important and generally causes a red shift.

The cell was evacuated at 653 K, right after heating. Two bands located at 2956 and 2856 cm^{-1} in the ν(CH) region show that a little methoxy still remained on the surface even after 60 min evacuation at 10^{-4} Torr, while methyl groups were then no longer appreciable (Fig. 4). The remarkable thermal stability of CH_3O on silica at this rather high temperature has been fully discussed earlier [28,37]. Neither methoxy moieties, nor formates, can survive onto Pd particles at this temperature [44,45]. Cell evacuation eliminated *ca.* 50% of the CO chemisorbed on the catalyst. The spectra in Fig. 4 also reveal that the remaining CO_S readily reacts with flowing H_2 at 523 K and that some water is formed in the process, probably because at this temperature the reaction mostly leads to methane under these conditions (high H_2/CO ratio and low pressure [37]), which is promptly swept from the surface.

$$CO + 3\,H_2 \rightarrow CH_4 + H_2O \quad (4)$$

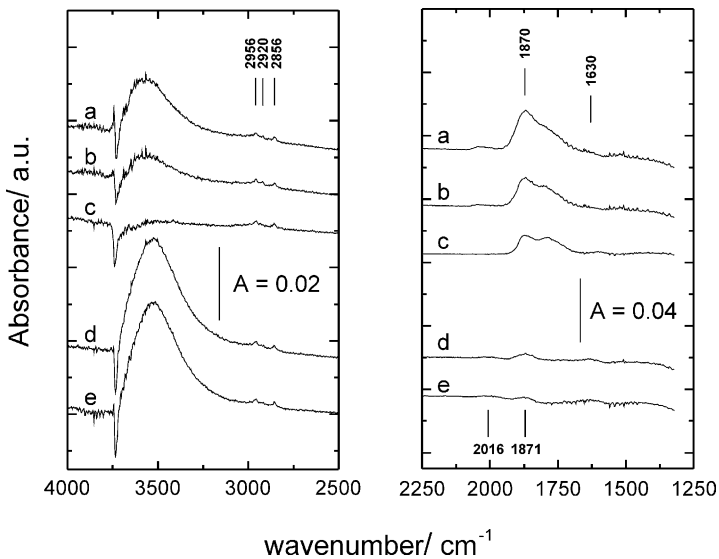

Fig. 4. Desorption of HCOOH from Pd/SiO_2 at: (a) 653 K, 10^{-1} Torr, 30 min; (b) 653 K, 10^{-3} Torr, 30 min and then cooling to (c) 523 K 10^{-4} Torr, 30 min, followed by reaction with flowing H_2 (100 cm^3/min) at 523 K for (d) 0.5 min, (e) 60 min.

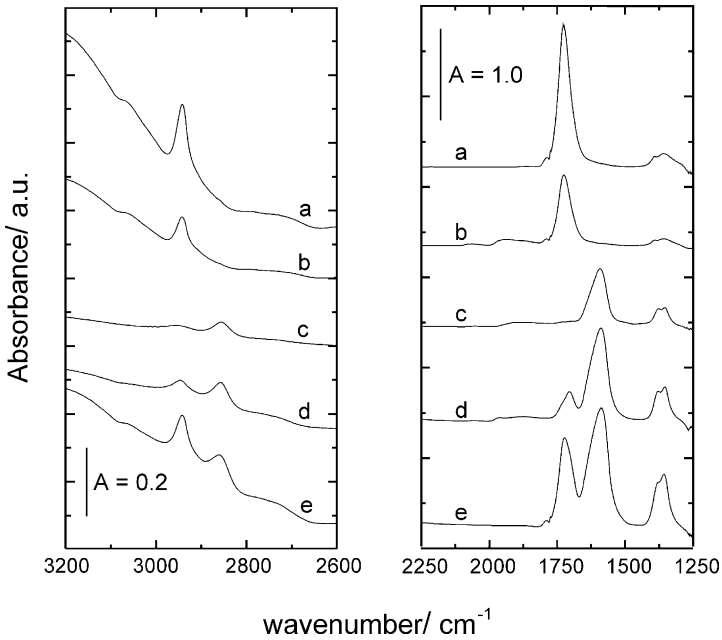

Fig. 5. Comparative infrared spectra of HCOOH (1 Torr) adsorbed at 298 K (0.5 min) on: (a) SiO_2; (b) MS0 (Pd/SiO_2); (c) MR5 (promoted Ca–Pd/SiO_2; calcium added to prereduced Pd metal particles); (d) MS5 (promoted Ca–Pd/SiO_2; calcium added to diammine palladium); (e) BS5 (blank of Ca/SiO_2). Samples were pretreated as described in Fig. 1.

Nevertheless, the residual methoxy groups could not be entirely removed by hydrogen, most likely because water does not chemisorb onto silica at high temperature and, so, cannot hydrolyze the Si–O bond.

3.2. Adsorption of formic acid on Ca-doped Pd/SiO_2

3.2.1. Adsorption on Ca-doped prereduced Pd/SiO_2

Fig. 5 (trace c) displays the spectrum of HCOOH dosed (1 Torr) at 298 K on the Ca-doped prereduced Pd/SiO_2 catalyst (coded MR5). Several, dramatic changes from the spectra taken after dosing formic acid onto the individual components of the surface (promoter, noble metal and support, also shown in Fig. 5), reveal the vast reactivity between the adsorbate and said surface components, and among them.

So, only bands at 2955–2940 (broad), 2856 and 2724 (vw) cm^{-1} can be seen in the ν(CH) region (the breadth of the band at 2955–2940 cm^{-1} is probably related to the presence of calcium). The signals at 3060 (formic acid dimer) and 2572 (condensed HCOOH) cm^{-1} are no longer present in the spectrum, which is consistent with the almost disappearance of the CO-stretching band characteristic of formic acid physisorbed onto silica in the low-frequency region (at 1725–1730 cm^{-1}) and the much lower intensity of the 2940 cm^{-1} band versus the one at 2856 cm^{-1}.

As expected, owing to the addition of the calcium promoter, appreciable amounts of b-HCOO were readily produced, but were partially consumed during the exposure time. A few m-HCOO was formed as well (see the tiny band at 1700 cm^{-1}), but it was readily depleted at room temperature (Fig. 6).

Chemisorbed CO, showing mono- and di-coordinated bands, which grew with time of exposure, was indicative, again, of the extensive decarbonylation of the adsorbed HCOOH on the Pd crystallites (Reaction 1). The amount of water observed, though, was much less than onto the unpromoted catalyst, Pd/SiO_2. The spectra in Fig. 6 also show CO_2(g) (2349 cm^{-1}), indicating that on this promoted catalyst the WGSR (Reaction 2) proceeds farther to the right than on Pd/SiO_2 (see later). Lastly, and in agreement with the extensive decomposition of HCOOH and the involvement of water in the WGSR, the loss of free OH groups of

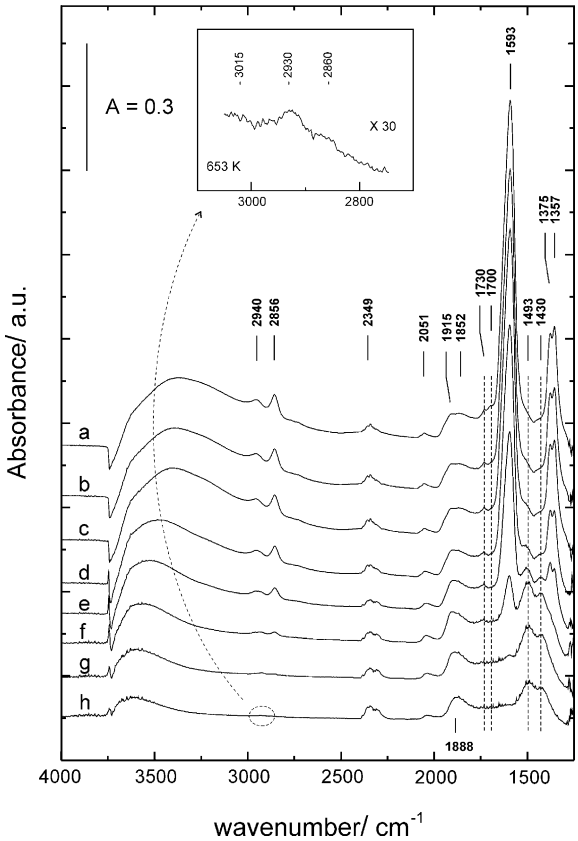

Fig. 6. Infrared spectra of HCOOH (1 Torr) adsorbed on MR5 (promoted Ca–Pd/SiO_2; calcium added to prereduced Pd metal particles; Ca/Pd = 2 at./at.) at increasing temperatures: (a) 298 K, 0.5 min; (b) 298 K, 10 min; (c) 298 K, 30 min; (d) 353 K; (e) 393 K; (f) 473 K; (g) 573 K and (h) 653 K, 30 min. The sample was pretreated as indicated in Fig. 1.

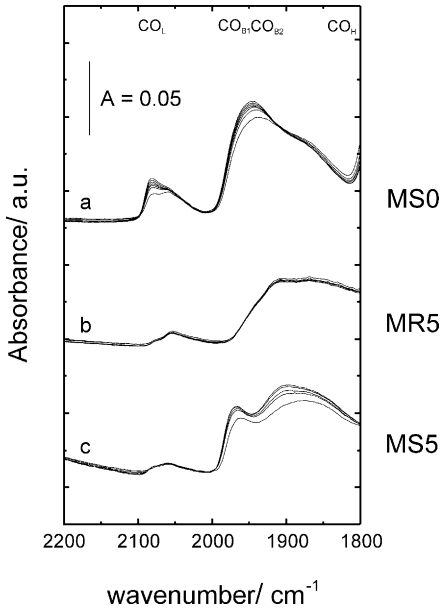

Fig. 7. Detail of the 2200–1800 cm^{-1} region of the FTIR spectra of HCOOH (1 Torr) adsorbed at 298 K on: (a) MS0 (Pd/SiO_2), (b) MR5 (promoted Ca–Pd/SiO_2; calcium added to prereduced Pd metal particles) and (c) MS5 (promoted Ca–Pd/SiO_2; calcium added to diammine palladium). Each set of spectra represent exposures during (upwards): 0.5, 5, 10, 15, 20 and 30 min, respectively; the full-range spectra are shown in Figs. 4, 6 and 9. Samples were pretreated as indicated in Fig. 1.

the silica surface on MR5 was 92% smaller than on the bare silica (on Pd/SiO_2 such loss was only about 30% less than on the support).

A closer view to the CO-stretching IR region reveals that, while on Pd/SiO_2 carbon monoxide chemisorbed and built-up with exposure time mostly on the open planes, corners and edges of the metal crystallites (Fig. 7), on MR5 the observed amount of CO chemisorbed on these surface sites was much less, as compared to that onto the (111) plane (both in linear and bridged forms) and, further, that no build-up of CO_S could be seen either. We believe that this dissimilar behavior is partially related (see later) to the broad background band in the 1870–1830 cm^{-1} region. This feature, which is only present on the Ca-promoted catalysts, has been reported to include a contribution from a convoluted band of CO C-bonded to Pd, while the oxygen atom is bonded to a promoter metal cation [27,46–48]. This 'background' signal, so, might well be the fingerprint of Ca–Pd intimacy, and reactivity, of the CaO_xH_y-doped Pd/SiO_2.

As no significant amount of CO_2 was observed at low temperatures on Pd/SiO_2 (Fig. 3), while carbon dioxide evolution on MR5 is evident, even at 298 K (Fig. 6), the combined effect of HCOOH decarbonylation and WGSR, which can be formally represented by the direct decarboxylation of the acid on the noble metal,

$$HCOOH \rightarrow CO_2 + H_2 \quad (5)$$

gives a simple (and plausible) clue to the kind of promoter–metal interaction existing on the catalyst surface: in MR5 CaO_xH_y-related formates are

decomposed by atomic hydrogen produced from HCOOH decarboxylation and then spilt-over from the Pd crystallites.

Formate decomposition progressed busily with heating on MR5, and almost nothing was left at 653 K (see the background signal around 1590 cm^{-1} and the small band at 2860 cm^{-1} in the ν(CH) region, Fig. 6). In comparison, a sizable portion of formate still remained on Ca/SiO_2 at this high temperature (Fig. 2).

Fig. 6 also shows the growth at increasing temperatures of two well resolved bands at 1493 and 1430 cm^{-1}. They have been assigned on bulk CaO_xH_y to the low-frequency vibration of the doubly degenerate asymmetric ν_3(CO) mode the free carbonate ion interacting with the oxide surface, to give "polydentate" and "simple" (symmetrical or non-coordinated) carbonates, respectively [49,50]. The onset of both signals is already discernible on MR5 at 298 K, which is consistent with former observations of Cabilla, who found these two types of surface species after dosing CO or CO_2 at RT onto these Ca-promoted Pd/SiO_2 catalysts [27]. Moreover, Cabilla's data showed that upon exposure to CO in the 298–653 K range, the band of polydentate carbonates (1493 cm^{-1}) was always more intense than that of the simple-carbonates (1430 cm^{-1}), as in Fig. 6, whereas the opposite was observed after dosing CO_2. These facts strongly suggest that the CO formed in the decarbonylation of HCOOH can promptly interact with the CaO_xH_y surface as well.

With heating, surface carbonates kept accumulating, while the remaining oxygenated species decomposed or desorbed. The maximum intensity of the carbonates IR bands was seen at ca. 473 K, after which both signals decayed too. At 653 K it was still possible to observe CO_2(g), together with a few CO(g) (2143 cm^{-1}) and chemisorbed CO, but no CH_4 (Fig. 6). Even though our IR signals are too weak to rule out the absence of CO bond scission, the addition of basic metal oxides as cocatalysts in the conversion of synthesis gas to methanol on supported Pd catalysts has been shown to inhibit CO dissociation [1,14,51,52] and, so, is not unexpected to have smaller, or undetectable, CH_4 peaks on MR5 than over the unpromoted Pd/SiO_2.

At higher temperatures, aside from the depletion of reactive CO_S on edges, corners and open planes on this catalyst already pointed out while analyzing the spectra at 298 K, the broad band of chemisorbed CO showed some distinct, qualitative changes from those on Pd/SiO_2: the terminal (CO_L) species desorbed (and/or decomposed) steadily, while the amount of CO_{B2} species (1912–1906 cm^{-1} signal) first increased (up to 473 K) and then decreased somewhat; its intensity at 653 K was about the same as it was at RT. The broad background signal centered around 1850 cm^{-1}, related to Ca–Pd closeness or intimacy, became significantly reduced with heating. All these features confirm that the Pd(1 1 1) planes are the least reactive of the metal surface.

In single crystal studies of formic acid adsorption, Aas et al. [53] reported that more CO_2 and H_2O are produced if palladium is oxygenated, as oxygen creates new adsorption sites for HCOOH, viz.

$$2\,HCOOH + O_{ads}{}^{2-} \rightarrow 2\,HCOO_{ads}{}^{-} + H_2O \qquad (6)$$

From this, one can say that oxygen presence (closeness of the Pd crystallites to CaO_xH_y) on MR5 could have partially prevented the formation of CO, favoring that of formates and water instead. Unfortunately, the latter is not entirely observable in our system, because the large amount of bidentate formate present on this promoted catalyst (and also on MS5, see later) masks the 1630 cm^{-1} band of water.

Evacuation down to 10^{-4} Torr at 653 K eliminated more than 60% of the chemisorbed CO, together with about 30% of the carbonates (Fig. 8). The shoulder in the spectra located at 1593 cm^{-1} and the combination band at 2930 cm^{-1} reveal, also, that some b-HCOO was still left, even after having submitted the catalyst to this thermal treatment in vacuo. Further exposure to flowing H_2 (at 523 K) gave some CO_S consumption, with water formation via Reaction 4, like on clean Pd/SiO_2. However, water production was much more pronounced on MR5, which is consistent with the additional decomposition of surface carbonates under flowing H_2 shown in Fig. 8.

$$CO_3{}^{2-} + H_2 \rightarrow CO_2 + H_2O \qquad (7)$$

3.2.2. *Adsorption on Ca-doped Pd-diammine/SiO_2*

In general terms, the adsorption and decomposition of formic acid at 298 K on this promoted catalyst (coded MS5) followed the same trends reported previously for MR5, where the calcium was added to prereduced Pd/SiO_2. Nevertheless, some of the observed spectral features were unique (Fig. 9).

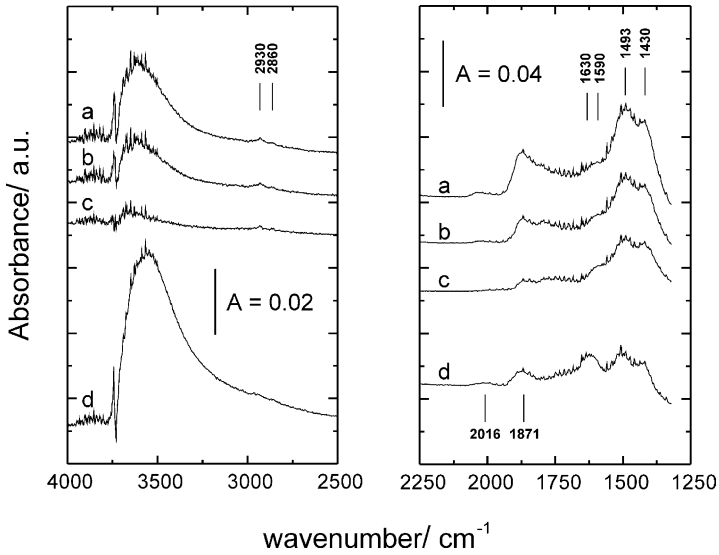

Fig. 8. Desorption of HCOOH from MR5 Ca–Pd/SiO_2 at: (a) 653 K, 10^{-1} Torr, 30 min; (b) 653 K, 10^{-3} Torr, 30 min and (c) 523 K 10^{-4} Torr, 30 min, followed by (d) reaction with flowing H_2 (100 cm^3/min) at 523 K, for 60 min.

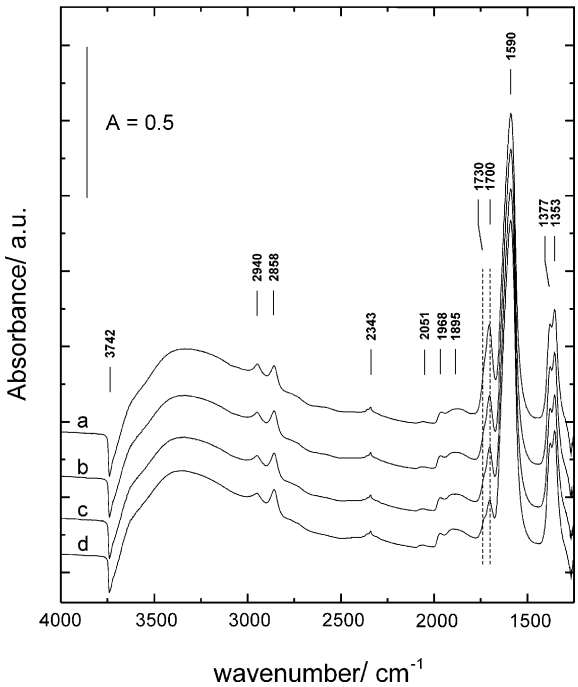

Fig. 9. Infrared spectra of HCOOH (1 Torr) adsorbed on MS5 (Promoted Ca–Pd/SiO_2; calcium added to diammine palladium; Ca/Pd = 2 at./at.) at 298 K, for (a) 0.5 min, (b) 5 min, (c) 15 min and (d) 30 min exposure. Sample was pretreated as indicated in Fig. 1.

As usual, the bands corresponding to physisorbed HCOOH (2940 and 1730 cm^{-1}) diminished with time of exposure, the latter being just a faint shoulder on the high frequency side of the prominent signal assigned to m-HCOO (1700 cm^{-1}). Monodentate formate was initially formed, in fairly large amount, but the species was continuously consumed afterwards. After 30 min the intensity of this band was only 40% of its initial value, but even then it was much stronger than on MR5. Conversely, all the IR bands attributed to b-HCOO (2858, 1590, 1377 and 1353 cm^{-1}) kept increasing with time and, actually, after 30 min of exposure the 1590 cm^{-1} band [ν_{as}(OCO)] was almost as intense as on the blank of Ca/SiO_2 (BS5).

Recalling that only formates annihilation was observed at RT on MR5 (Fig. 6), this diminution of the m-HCOO signal and concomitant increase of the b-HCOO band at 298 K on MS5 reveal that the latter formates are more stable and/or less reactive species. More importantly, we believe these moderate changes on MS5 are indicative (and a consequence) of important structural differences between both promoted catalysts, viz. Using TEM, the Pd metal crystallites on MS5 showed a bimodal distribution and, on average, the exposed metal fraction of palladium was lower on MS5 than on MR5 (Table 1). In addition, we found employing HRTEM, that because of the

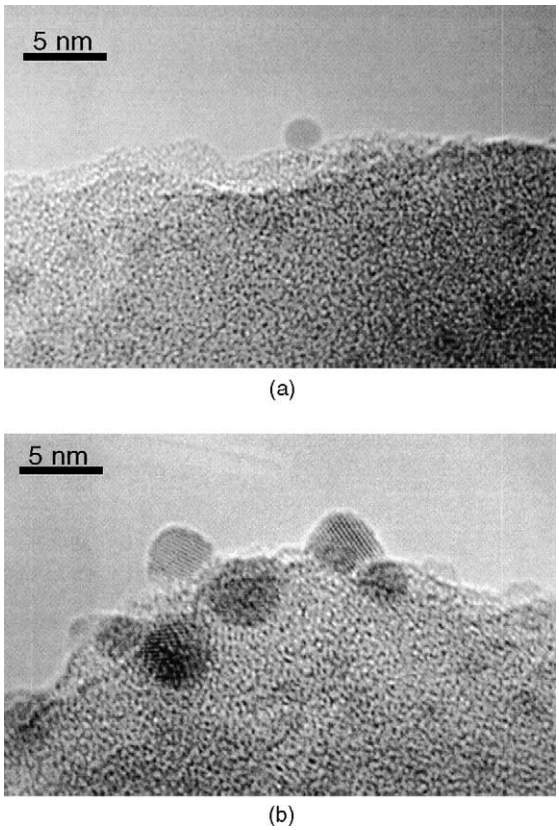

Fig. 10. HRTEM micrographs of reduced samples of the Pd/SiO_2 (MS0) and Ca–Pd/SiO_2 (MS5) catalysts. The micrographs were taken in a JEOL-2000-EX microscope, with a structural resolution of 0.21 nm [12].

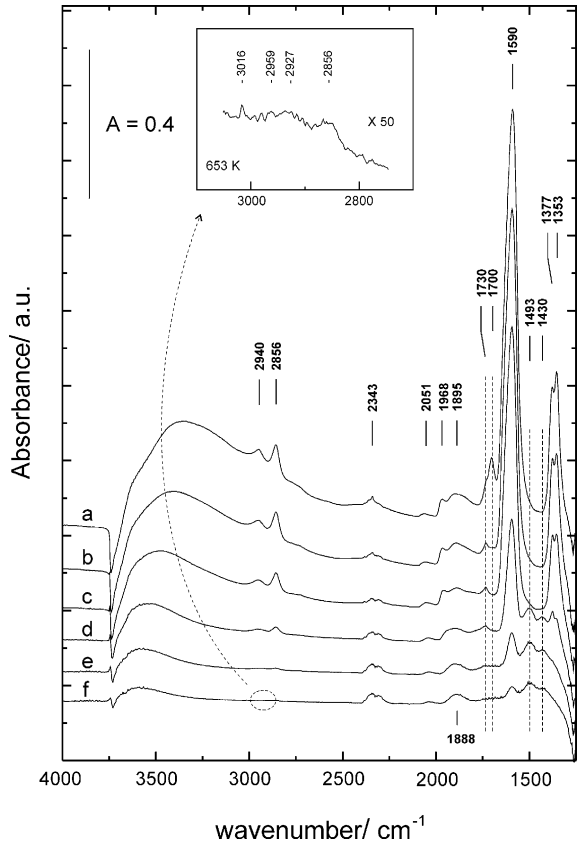

Fig. 11. Spectra of HCOOH (1 Torr) adsorbed on MS5 at increasing temperatures: (a) 298 K, 30 min; (b) 353 K; (c) 393 K; (d) 473 K; (e) 573 K and (f) 653 K, 30 min. Sample was pretreated as indicated in Fig. 1.

preparation method the larger metal particles on MS5 are 'decorated' with CaO_xH_y [12] (compare the size and contact angle of these crystallites with those of Pd/SiO_2 in Fig. 10). Lastly, while the buildup of chemisorbed CO was negligible on MR5 this buildup was, instead, quite appreciable on MS5, with considerable amount of the reactive CO_{B1} (1960–1970 cm^{-1}) accumulating on the Pd surface rather than being consumed (Fig. 7).

Plausibly, then, owing to the decoration of part of the Pd crystallites in MS5 with CaO_xH_y, which can 'block' surface migration of adsorbates/reactants, formic acid chemisorbed (as formates) onto patches of calcium oxyhydroxide laying nearby onto the silica support, cannot be reached by atomic hydrogen formed on the Pd crystallites by HCOOH decarbonylation/WGSR. In other words: owing to the mechanical, blocking effect of CaO_xH_y, atomic hydrogen cannot spill-over to annihilate formates on MS5 (then the initial build-up of m-HCOO on the adjacent CaO_xH_y/silica patches) as readily as it does on MR5 where, by design, no obstacle to hydrogen spillover was set.

Fig. 11, which shows the development of surface species on MS5 upon heating, further illustrates about the blocking effect of the CaO_xH_y that decorates the Pd crystallites. Each and every one of the desorption/decomposition processes already described when considering the heating of the prereduced Ca-Pd/SiO_2 catalyst (MR5) is again discernible. Said processes, however, always occurred either at higher temperature (e.g., the appearance of carbonates at 473 K instead of 298 K on MS5, respectively, MR5), or were of

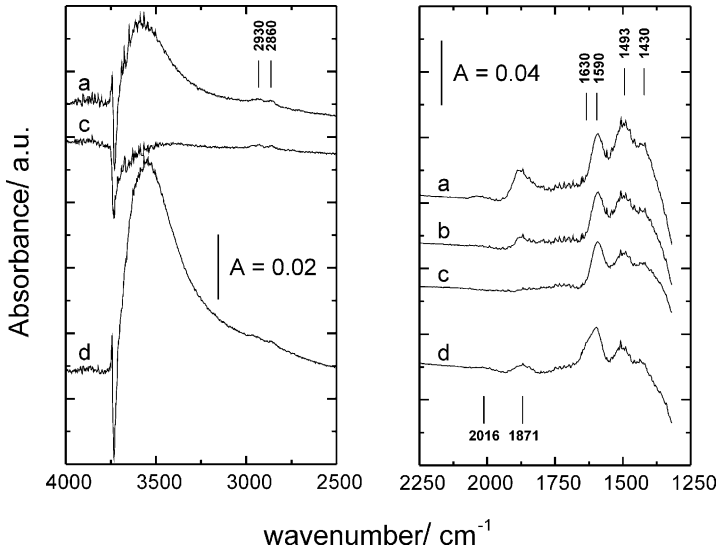

Fig. 12. Desorption of HCOOH from MS5 Ca–Pd/SiO_2 at: (a) 653 K, 10^{-1} Torr, 30 min; (b) 653 K, 10^{-3} Torr, 30 min and (c) 523 K 10^{-4} Torr, 30 min, followed by (d) reaction with flowing H_2 (100 cm^3/min) at 523 K, for 60 min.

less magnitude (e.g., some unreacted b-HCOO was still present at 653 K on the Ca-doped diammine Pd/SiO_2, while none was appreciable on the prereduced Ca–Pd/SiO_2).

Indeed, aside from the fact that we could only observe surface carbonates on the Ca-Pd/silica catalysts, but not on Pd/SiO_2 (which implies that the HCOOH → CO → CO_2 pathway is mediated by the presence of both the noble metal and the promoter), the whole qualitative picture on these promoted materials constitutes a remarkable combination of the spectra of the blank of Ca/SiO_2 (BS5, Fig. 2) and the clean Pd/SiO_2 (MS0, Fig. 3). Interestingly, methane/methyl formation followed the sequence MS0 > MS5 > MR5, probably because much less (highly reactive) bridged CO_{B1} was left on the last one by the time the heating ramp reached typical syn-gas process temperatures ($T > 523$ K).

The residual amount of chemisorbed species after evacuating down to 10^{-4} Torr at high temperature (Fig. 12) was somewhat different on MR5 versus MS5: carbonate decomposition was larger, and almost no CO_S was left on the latter. Because it is well-known that evacuating at 653 K can only partially desorb carbon monoxide, it is highly likely that the closeness (or intimate contact) between the CaO_xH_y decorating particles and the Pd crystallites in MS5 can favor further progress of the WGSR on this catalyst, with the calcium oxyhydroxide phase readily supplying mobile water. More importantly, the evacuation treatment did not remove any remaining b-HCOO, nor did the exposure of the MS5 catalyst to flowing hydrogen at 523 K. Again, the impact of the H_2 treatment on MS5 was intermediate between those of the clean Pd/silica and the Ca-doped prereduced Pd/SiO_2 catalysts.

4. Conclusions

Formic acid physisorbs on SiO_2 at room temperature, with partial dimerization and condensation, and extensive hydrogen bonding of the sorbed species. At higher temperatures all these infrared signals decrease in intensity, and the dimer disappears. From 473 K onwards (up to 653 K) a new, weak band at 1590 cm^{-1}, corresponding to the ν_{as}(OCO) of bidentate formate, reveals that a few HCOOH is able to decompose on the silica support, with further reduction to methoxy. Upon evacuation at 653 K, these surface CH_3O are stable.

On the unpromoted catalyst, Pd/SiO_2, formic acid physisorbs and reacts at 298 K. About 50% of the adsorbate undergoes decarbonylation, yielding CO (which chemisorbs onto the metal crystallites in linear and bridged forms), and hydrogen; a little b-HCOO

is observed as well. With heating, both HCOOH and carbon monoxide react with the H_2 produced in the decarbonylation, to give adsorbed methanol (methoxy), and CH_4 (and methyl) at 653 K. Formic acid decomposition is accompanied by some water gas shift (WGSR) as well.

Extensive surface bidentate formate was observed on the blank of CaO_x/SiO_2, upon adsorbing HCOOH (1 Torr) at 298 K, with very intense IR signals neatly showing up in the full temperature range (298 to 653 K). The amount of b-HCOO partially decreased on evacuation, but remained almost unchanged when hydrogen was flown, at 523 K.

Monodentate formate, together with sorbed HCOOH, chemisorbed CO (from the decarbonylation of the adsorbate on the Pd crystallites) and CO_2(g) (from the WGS reaction) were observed on both calcium-promoted Pd/silica catalysts when these materials were exposed to 1 Torr of formic acid at RT. At increasing temperatures, b-HCOO, carbon dioxide and carbonates (polydentate and simple) were formed, but hardly any methane, nor methyl, was observed. On MR5 (promoted Ca–Pd/SiO_2 with calcium added to prereduced Pd metal particles) the extension and/or onset of all these processes was more frank than on MS5 (promoted Ca–Pd/SiO_2; calcium added to diammine palladium), most likely owing to the combined impact of a higher dispersion of the palladium crystallites on the former preparation, and calcium oxyhydroxide decoration (CaO_xH_y) of the metal particles on the latter.

Unfortunately, although less CO scission was observed in these calcium-promoted catalysts versus the clean Pd/SiO_2, in agreement with our reaction data at 2.5–3 MPa and 523–553 K (in which conditions much more methanol was produced, with improved selectivity to oxygenates [12,27]), the present FTIR study was unable to tell whether b-HCOO is a key intermediate and/or rate determining step in methanol synthesis on these CaO_x-Pd/SiO_2 catalysts or just a mere spectator.

Acknowledgements

Thanks are given to Eduardo A. Moreira for his skilled technical assistance. The financial support of Universidad Nacional del Litoral (UNL), Consejo Nacional de Investigaciones Científicas y Técnicas (CONICET) and Programa de Modernización Tecnológica (ANPCyT) is gratefully acknowledged.

References

[1] Y. Kikuzono, S. Kagami, S. Naito, R. Onishi, K. Tamaru, Faraday Disc. Chem. Soc. 72 (1982) 135.
[2] H. Orita, S. Naito, K. Tamaru, J. Catal. 90 (1984) 183.
[3] J.H. Lunsford, Chem. Ind. 22 (1985) 95.
[4] J.M. Driessen, E.K. Poels, J.P. Hindermann, V. Ponec, J. Catal. 82 (1983) 26.
[5] J.S. Rieck, A.T. Bell, J. Catal. 96 (1985) 88.
[6] H. Deligianni, R.L. Mieville, J.B. Peri, J. Catal. 95 (1985) 465.
[7] P.J. Berlowitz, D.W. Goodman, J. Catal. 108 (1987) 364.
[8] F. Solymosi, A. Erdöheli, M. Lancz, J. Catal. 95 (1985) 567.
[9] G.C. Chinchen, P.J. Denny, J.R. Jennings, M.S. Spencer, K.C. Waugh, Appl. Catal. 36 (1988) 1, and references therein.
[10] A.L. Bonivardi, M.A. Baltanás, D.L. Chiavassa, Stud. Surf. Sci. Catal. 75(B) (1993) 801.
[11] A. Gotti, R. Prins, J. Catal. 175 (1998) 302.
[12] A.L. Bonivardi, D.L. Chiavassa, M.A. Baltanás, G.A. Cifredo, S. Bernal, in: Proceedings of the 11th International Congress on Catalysis, Baltimore, 1996, Po-083.
[13] A.L. Bonivardi, D.L. Chiavassa, M.A. Baltanás, Stud. Surf. Sci. Catal. 114 (1998) 533.
[14] A.F. Gusovius, T.C. Watlin, R. Prins, Appl. Catal. A: Gen. 188 (1999) 87.
[15] A.L. Bonivardi, M.A. Baltanás, J. Catal. 138 (1992) 500.
[16] D.L. Chiavassa, M.Sc. Thesis, Universidad Nacional del Litoral, Santa Fe, Argentina, 1998.
[17] A.L. Bonivardi, M.A. Baltanás, J. Catal. 125 (1990) 243.
[18] G.J. Millar, C.H. Rochester, K.C. Waugh, J. Chem. Soc. Faraday Trans. 87 (9) (1991) 1491.
[19] G. Herzberg, Molecular Spectra and Molecular Structure. Part II. Infrared and Raman Spectra of Polyatomic Molecules, Van Nostrand, New York, 1945.
[20] C. Houtman, M. Barteau, Surf. Sci. 248 (1991) 57.
[21] D.M. Monti, N.W. Cant, D.L. Trimm, M.S. Wainright, J. Catal. 100 (1986) 17.
[22] R. Burch, S. Chalker, J. Pritchard, J. Chem. Soc. Faraday Trans. 87 (1) (1991) 193.
[23] A. Ueno, T. Onishi, K. Tamaru, Trans. Faraday Soc. 67 (1971) 3585.
[24] A. Palazov, G. Kadinov, Ch. Bonev, D Shpov, J. Catal. 74 (1982) 44.
[25] C. Binet, J.C. Lavalley, J. Chim. Phys. 89 (1992) 1779.
[26] T. Shimanouchi, Tables of Molecular Vibrational Frequencies Consolidated, National Standards of Reference Data Services, vol. 1, National Bureau of Standards, Washington, DC, USA, 1972.
[27] G.C. Cabilla, Doctoral Dissertation, Universidad Nacional del Litoral, Santa Fe, Argentina, 2000.
[28] F. Raskó, J. Bontovics, F. Solymosi, J. Catal. 146 (1994) 22.
[29] F. Le Peltier, P. Chaumette, J. Saussey, M.M. Bettahar, J.C. Lavalley, J. Mol. Catal. A: Chem. 122 (1997) 131.

[30] J. Cai, Y. Liao, H. Chen, K.R. Tsai, Stud. Surf. Sci. Catal. 75(C) (1993) 2769.
[31] N. Nomura, T. Tgawa, S. Goto, Appl. Catal. A: Gen. 166 (1998) 321.
[32] P.G. Gopal, R.L. Schneider, K.L. Watters, J. Catal. 105 (1987) 366.
[33] C. Schild, A. Wokaun, A. Baiker, J. Mol. Catal. 63 (1990) 223.
[34] R.P. Young, Can. J. Chem. 47 (1969) 2237.
[35] B.E. Hayden, K. Prince, D.P. Woodruff, A.M. Bradshaw, Surf. Sci. 133 (1983) 589.
[36] B.E. Hayden, K. Prince, P. Woodruff, A.M. Bradshaw, Phys. Rev. Lett. 51 (1983) 475.
[37] G.C. Cabilla, A.L. Bonivardi, M.A. Baltanás, J. Catal. 201 (2001) 213.
[38] S.W. Jorgensen, R.J. Madix, J. Am. Chem. Soc. 110 (1988) 397.
[39] D. Sandler, W. Erley, J. Vac. Sci. Technol. A 8 (4) (1990) 3357.
[40] C. Cabilla, A.L. Bonivardi, M.A. Baltanás, Catal. Lett. 55 (1998) 147.
[41] E. Borello, A. Zecchina, C. Morterra, J. Phys. Chem. 71 (1967) 2938.
[42] K. Raskó, J. Bontovics, F. Solymosi, J. Catal. 143 (1993) 138.
[43] A. Fischer, A.T. Bell, J. Catal. 184 (1999) 357.
[44] L. Davis, M.A. Barteau, Surf. Sci. 255 (1990) 235.
[45] L. Davis, M.A. Barteau, Surf. Sci. 256 (1991) 50.
[46] S.S. Boujana, D. Demri, A. Cressely, A. Kiennemann, J.P. Hindermann, Catal. Lett. 7 (1990) 359.
[47] V. Pitchon, M. Primet, H. Praliaud, Appl. Catal. 62 (1990) 317.
[48] A. Bonivardi, C. Pistonesi, M. Menghini, A. Juan, Comput. Mater. Sci. 18 (2000) 39.
[49] G. Busca, V. Lorenzelli, Mater. Chem. 7 (1982) 89, and references therein.
[50] F.A. Andersen, L. Brecevic, Acta Chem. Scandin. 45 (1991) 1018.
[51] R.F. Hicks, A.T. Bell, J. Catal. 91 (1985) 104.
[52] J.S. Rieck, A.T. Bell, J. Catal. 100 (1986) 305.
[53] N. Aas, Y. Li, M. Bowker, J. Phys.: Condens. Matter 3 (1991) CS281.